Journal of Thermal Analysis, Vol. 52 (1998) 631-656

COMPUTATION OF HEAT CAPACITIES OF SOLIDS USING A GENERAL TARASOV EQUATION

M. Pyda[1], *M. Bartkowiak*[2] *and B. Wunderlich*[1*]

[1]Department of Chemistry, The University of Tennessee, Knoxville TN 37996-1600 and Chemical and Analytical Sciences Division, Oak Ridge National Laboratory Oak Ridge TN 37831-6197
[2]Department of Physics and Astronomy, The University of Tennessee Knoxville TN 37996-1200 and Solid State Div., Oak Ridge National Laboratory Oak Ridge TN 37831-6030, USA

Abstract

The general Tarasov function is fitted to the skeletal heat capacities of materials with widely different crystal structures. Examples are chosen from flexible macromolecules (polyethylene, polypropylene, poly(ethylene terephthalate), selenium, rigid macromolecules (diamond and graphite), and a small molecule (fullerene, C_{60}). A new optimization approach using the Mathematica™ software is developed. It results in one-, two-, and three-dimensional Debye temperatures, Θ_1, Θ_2 and Θ_3 the fitting parameters of the Tarasov function. In addition to the Tarasov function, the evaluation of the heat capacities makes use of approximate group-vibrational spectra. The results support the earlier assumption that $\Theta_2=\Theta_3$ for simple, solid, linear macromolecules. In more complicated bonding situations, Θ_1, Θ_2 and Θ_3 are used as averaging fitting parameters. This general approach provides an improvement in the quantitative thermal analyses of polymers and other substances included in the ATHAS Data Bank. Sufficient programming information is provided to enable anyone the computation with a copy of the popular Mathematica™ software. The programming file is also downloadable from the WWW.

Keywords: diamond, fullerene, graphite, heat capacity, polyethylene, poly(ethylene terephthalate), polypropylene, selenium, solid state, Tarasov equation, vibrational spectra

Introduction

A general description of the heat capacity of macromolecules and complex, small molecules in the solid state is rather difficult if one wants to cover a large range of temperature. This problem has been addressed frequently [1–4]. To approach reality, models for the macroscopic, measured heat capacity must estab-

* Author to whom all correspondence should be addressed.

1418–2874/98/ $ 5.00

Akadémiai Kiadó, Budapest
Kluwer Academic Publishers, Dordrecht

lish a link to the microscopic molecular motion as expressed by its vibrational spectrum. At lower temperatures, vibrational motion provides practically the only contribution to the heat capacity. As the temperature increases, large-amplitude conformational, rotational, and translational motions may also add to the heat capacity. The deviation of the measured heat capacity from the baseline of the vibrational contributions permits the assessment of the large-amplitude motions, responsible for most changes in mechanical properties. In addition, it permits a quantitative identification of broad glass, melting, and disordering transitions. Therefore, calculation of the vibration–only heat capacity is crucial for quantitative thermal analysis. The full vibrational spectrum, however, is often not available and never sufficiently precise in the low-frequency region for an inversion to heat capacity. Hence, a series of approximations have been developed for computation of heat capacities of sufficient precision. All approaches are based on the classical Einstein [5] and Debye treatments [6]. The heat capacity of many simple solids, such as metals and salts can even be described by a single, three-dimensional Debye function with only one parameter, the Debye temperature Θ_D [7]. For more complicated, covalent molecular structures more detailed, full, albeit approximate, vibrational spectra are necessary and must be treated as first proposed by Born and von Kármán [8].

Using the Advanced Thermal Analysis System (ATHAS) we have been successful in describing the heat capacity of solid, linear macromolecules using an approximation of the vibrational spectrum [9]. In this approach the vibrational heat capacity at low temperatures is arbitrarily separated into two independent contributions: one, the low-frequency portion, coming from the skeletal; the other, the high-frequency portion, from the group vibrations. The former is approximated by the simple Tarasov function that describes heat capacities of chain molecules with two parameters, the characteristic temperatures Θ_1 and Θ_3 [10]. The latter is derived from the known group vibrations, inverted to heat capacities using the Einstein function for narrow distributions of frequencies and a combination of Einstein functions and simple box-distributions for broader frequency regions [11]. Information on thermodynamic properties of currently nearly 250 linear macromolecules and small molecules have been assessed using this approach and are collected in the ATHAS Data Bank [12].

The heat capacities of diamond, graphite, and selenium have been characterized [13] using more general forms of the Tarasov functions [14]. For example, in order to fit the skeletal heat capacity of graphite, the Tarasov equation was used as a combination of two- and three-dimensional Debye functions (characteristic temperatures Θ_2 and Θ_3). Multiple Tarasov functions were used for the distinction between two- and three-dimensional crystal structures of group IV chalcogenides [15]. Better fits of the skeletal heat capacities can naturally be achieved using more fitting parameters. The general Tarasov equation [14], for example, involves a combination of one-, two-, and three-dimensional Debye functions (three fitting parameters, Θ_1, Θ_2, Θ_3). Separate Tarasov functions for longitudinal and transverse vibrations can further double these parameters [15],

and choosing independent numbers of vibrators in the general Tarasov equation can lead up to five fitted parameters for a single Tarasov fit (Θ_1, Θ_2, Θ_3, N_1, N_2, N_3, with $N_1+N_2+N_3$=total number of skeletal vibrations, N_{sk}). Previously such multiple parameter fitting was done by trial and error because of difficulties in the inversion of the Debye function that cannot be integrated in closed form. A fitting scheme that can be extended to multiple parameters will be described in this paper, making use of the general Tarasov equations. The results will be discussed in light of the known properties of frequency spectra. As examples, we consider diamond, graphite, and fullerene (C_{60}) as examples of the large structural variation possible among the allotropes of carbon, and several flexible macromolecules: polyethylene (PE), polypropylene (PP), poly(ethylene terephthalate) (PET), and selenium (Se). Combinations of small and large motifs within the same molecule, as are found in stiff-chain macromolecules will be discussed separately in a later publication.

In an Appendix, the general computer program is given, prepared in Mathematica™ programming language [16]. This program can also be found in and downloaded from our World Wide Web home page [17] and run on personal computers with existing Mathematica™ software [18].

Calculation of the heat capacity for the solids

Calculation of the vibrational heat capacity is based on low-temperature, experimental heat capacity at constant pressure, C_p(exp). These are converted to heat capacity at constant volume C_V(exp) using the standard thermodynamic relation involving compressibility and expansivity. If these additional experimental data are not available, one can make use of the Nernst-Lindemann approximation [19, 20].

$$C_p(\text{exp}) - C_V(\text{exp}) = 3RA_o\frac{C_p^2(\text{exp})}{C_V(\text{exp})}T/T_m \quad (1)$$

where A_o, is close to a universal constant and can be taken as ≈0.0039 K mol J^{-1}; T is the temperature; T_m, the equilibrium melting temperature; and R, the gas constant.

Assuming that C_V(exp) contains only vibrational contributions, it can be separated into the heat capacities from group vibrations C_V(gr) and skeletal vibrations C_V(sk):

$$C_V(\text{exp}) = C_V(\text{gr}) + C_V(\text{sk}) \quad (2)$$

The C_V(gr) is computed using frequency spectra obtained from the analysis of infrared and Raman spectra and is, for computational purposes, further divided as follows:

$$C_V(\text{gr}) = C_V(\text{box}) + C_V(\text{Einstein}) \quad (3)$$

where C_V(box) is the part of the heat capacity linked to parts of the spectrum represented by box-like distribution functions, and C_V(Einstein) is the heat capacity contribution best approximated by separate Einstein modes. For the latter one can write:

$$C_V(\text{Einstein})/NR = \sum_i \mathbf{E}(\Theta_{E_i}/T) = \sum_i \frac{(\Theta_{E_i}/T)^2 \exp(\Theta_{E_i}/T)}{[\exp(\Theta_{E_i}/T)-1]^2} \quad (4)$$

with $\Theta_{E_i}=h\nu_i/k$, representing the given Einstein frequencies in kelvin, and h and k are Planck's and Boltzmann's constants, respectively. A typical collection of Einstein modes is schematically shown in Fig. 1A. It represents the 4.59 Einstein modes of polyethylene listed in Table 1.

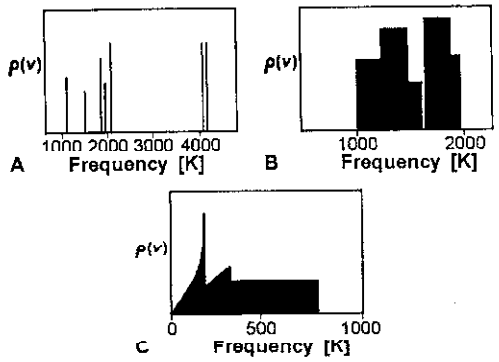

Fig. 1 (A) Frequency spectrum of the Einstein modes of Table 1; (B) The same for the box distributions in Table 1; (C) Schematic of the frequencies distribution of the general Tarasov function, Eq. (6)

The expression C_V(box) is given by a sum over the identified areas of the vibrational spectrum which can be represented by box-like spectra, as illustrated in Fig. 1B for polyethylene. The five frequency regions are listed also in Table 1. Each box is represented by a sum of one-dimensional Debye functions $\mathbf{D}_1$ and corresponds to uniformly distributed vibrations within the frequency interval from Θ_U to Θ_L [11]:

$$C_V(\text{box})/NR = \mathbf{B}(\Theta_U/T,\Theta_L/T) = \frac{\Theta_U}{\Theta_U-\Theta_L}[\mathbf{D_1}(\Theta_U/T)-(\Theta_L/\Theta_U)\mathbf{D_1}(\Theta_L/T)] \quad (5)$$

After subtracting the group vibration contributions from C_V(exp), the experimental C_V(sk) remains and is fitted at low temperatures to the general Tarasov function **T** [13, 14]:

$$C_V(\text{sk})/NR = \mathbf{T}(\Theta_1/T,\Theta_2/T,\Theta_3/T) =$$

$$\mathbf{D_1}(\Theta_1/T) - (\Theta_2/\Theta_1)[\mathbf{D_1}(\Theta_2/T) - \mathbf{D_2}(\Theta_2/T)] - (\Theta_3^2/\Theta_1\Theta_2)[\mathbf{D_2}(\Theta_3/T) - \mathbf{D_3}(\Theta_3/T)] \quad (6)$$

to obtain the three characteristic parameters Θ_1, Θ_2, and Θ_3 that represent the maximum frequencies of the corresponding distribution. Figure 1C illustrates the frequency distribution of Eq. (6) for an arbitrary set of parameters. The functions $\mathbf{D_1}$, $\mathbf{D_2}$ and $\mathbf{D_3}$ are the one-, two-, and three-dimensional Debye functions, respectively [6, 21]:

$$C_V/NR = \mathbf{D_1}(\Theta_1/T) = (T/\Theta_1)\int_0^{(\Theta_1/T)} \frac{(\Theta/T)^2\exp(\Theta/T)}{[\exp(\Theta/T) - 1]^2} d(\Theta/T) \quad (7)$$

$$C_V/NR = \mathbf{D_2}(\Theta_2/T) = 2(T/\Theta_2)^2\int_0^{(\Theta_2/T)} \frac{(\Theta/T)^3\exp(\Theta/T)}{[\exp(\Theta/T) - 1]^2} d(\Theta/T) \quad (8)$$

$$C_V/NR = \mathbf{D_3}(\Theta_3/T) = 3(T/\Theta_3)^3\int_0^{(\Theta_3/T)} \frac{(\Theta/T)^4\exp(\Theta/T)}{[\exp(\Theta/T) - 1]^2} d(\Theta/T) \quad (9)$$

where N denotes the number of the vibrational modes for the frequency distribution. Figure 2 illustrates the three frequency distributions of the Debye functions. It is of interest to note that the combinations of the three Debye functions for the general Tarasov function, shown in Fig. 1C, are chosen such that each section of

Table 1 Approximate Frequency Spectrum for Polyethylene Group Vibrations[a]

Vibration type		Frequency in K	Number of Vibrators
CH_2 asym. stretch	Θ_E	4148.1	1.00
CH_2 sym. stretch	Θ_E	4097.7	1.00
CH_2 bending	Θ_E	2074.7	1.00
CH_2 wagging	Θ_L,Θ_U	1698.3, 1976.6	0.65
CH_2 wagging	Θ_E	1976.6	0.35
CH_2 twisting/rocking	Θ_L,Θ_U	1689.6, 1874.3	0.48
CH_2 twisting/rocking	Θ_E	1874.3	0.52
C–C-stretching	Θ_L,Θ_U	1377.6, 1637.5	0.34
C–C-stretching	Θ_L,Θ_U	1377.6, 1525.4	0.35
C–C-stretching	Θ_E	1525.4	0.31
CH_2 rocking/twisting	Θ_E	1494.1	0.04
CH_2 rocking/twisting	Θ_L,Θ_U	1038.0, 1494.1	0.59
CH_2 rocking/twisting	Θ_E	1079.1	0.37

[a] Fitted to dispersion curve of J. Barnes and B. Fanconi, J. Phys. Ref. Data, 7 (1978) 309.

the lower frequency distribution which is replaced by a higher-level Debye function has the same number of vibrators as the lower-level Debye function would have had in this frequency region on extension to zero. By this assumption the number of fitting parameters is reduced from five to three, as pointed out above.

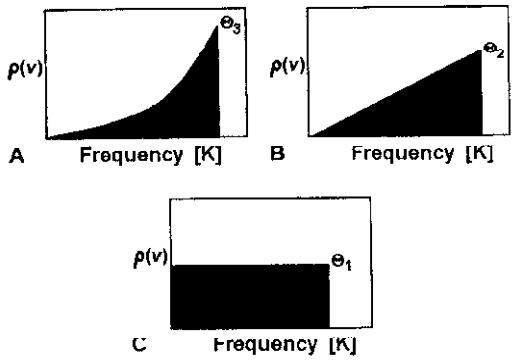

Fig. 2 Frequency distributions for (A) one-dimensional, (B) two-dimensional, (C) three-dimensional Debye Functions (Eqs (7)–(9))

The optimization method used to obtain Θ_1, Θ_2 and Θ_3 is based on minimizing the chi-square statistic function (χ^2):

$$\chi^2 = \sum_i \left[\frac{C_V(\mathrm{sk})_{\mathrm{exp}}(T_i) - C_V(\mathrm{sk})_{\mathrm{calc}}(T_i,\Theta_3,\Theta_2,\Theta_1)}{\sigma_i} \right]^2 \qquad (10)$$

where σ_i is the standard deviation of the experimental data taken at temperatures T_i. Low values of χ^2 correspond to an overall better fitting of the calculated heat capacity to the experimental data. The numerical minimization is conveniently performed with a personal computer within the programming language of Mathematica™ [16] by the built-in function 'FindMinimum,' and therefore, is particularly easy to use. Another advantage is that all three Debye functions are calculated within the Mathematica™ software with help of the Jouquiere function and the Riemann zeta-function. Such method of fitting was discussed before, but based on a main-frame computer program using the Fortran Math Library of the Numerical Algorithm Group (NAG), not easily available for every thermal analyst [22].

The values of Θ_1, Θ_2 and Θ_3 which best fit the experimental data can then be used to obtain the calculated heat capacity at constant volume C_V(calc) as the sum of the skeletal and group contributions, as indicated in Eq. (2). The C_V(calc) is finally converted back to C_p(calc) with Eq. (1), to obtain the vibration-only heat capacity over a temperature range exceeding the fitting range.

The new approach to link heat capacity to the vibrational spectrum is more general than used previously in the ATHAS analysis for polymers and it elimi-

nates the trial-and-error fitting of the Θ-temperaturesas shown schematically in Fig. 3. For all linear macromolecules it was assumed that $\Theta_2=\Theta_3$, so that the general Tarasov Eq. (6) reduces to:

$$C_V(sk)/NR = T(\Theta_1/T,\Theta_3/T) = D_1(\Theta_1/T) - (\Theta_3/\Theta_1)[D_1(\Theta_3/T) - D_3(\Theta_3/T)] \quad (11)$$

as originally proposed by Tarasov for chain molecules [1, 10, 23]. The possibility of a significant contribution to the heat capacity of vibrations distributed as in a two-dimensional continuum was thus excluded. The other possible simplification, using Eq. (6) without the one-dimensional continuum, was applied when discussing layer structures [10, 15, 23–25]. In this case Θ_1 is assumed to be equal to Θ_2, eliminating the one-dimensional contribution in Fig. 1C.

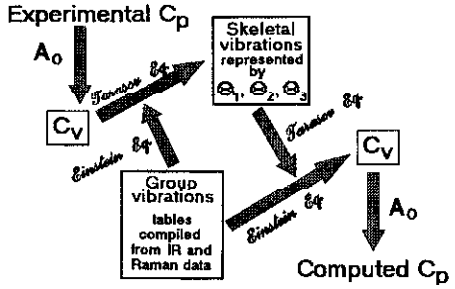

Fig. 3 ATHAS Scheme for the calculation of heat capacities of solids

At very low temperatures all Tarasov functions coincide with the three-dimensional Debye function and lead to the well-known T^3 temperature dependence of the heat capacity:

$$\Theta_D = \sqrt[3]{\Theta_1\Theta_2\Theta_3} \quad (12)$$

The pure one-, two-, and three-dimensional Debye functions, as given in Eqs (7)–(9), are recovered from Eq. (6) with $\Theta_2=\Theta_3=0$, $\Theta_3=0$ and $\Theta_1=\Theta_2$, and $\Theta_1=\Theta_2=\Theta_3$, respectively.

Results

Four polymers: PE, PP, PET, and selenium and three allotropes of carbon: diamond, graphite, and fullerene (C_{60}) were analyzed using the new optimization approach of the general Tarasov Eq. (6) as detailed in the Appendix. The experimental data of C_p(exp), the parameters for Eq. (1), and the approximate group vibration spectra were taken from literature and from the ATHAS data bank [12]. For PE, C_p(exp) and the group vibrational spectrum, as listed in Table 1, agrees with the data used in Ref. [26]. For PP C_p(exp) and the group vibration approximation were derived first in Ref. [27], and for PET, in Ref. [28]. The temperature ranges of the fitting of the experimental data to Eq. (6) are listed in Table 2.

Table 2 Results of Θ_1, Θ_2, Θ_3 fit and parameters that have been used for the C_V calculation[a]

Sample and range of temperature fit	N_{gr} (#)	N_{sk} (#)	T_m^o / K	Θ_1/ K	Θ_2/ K	Θ_3/ K
PE	7	2	414.6	547.5	146.7	146.7
(0.1–270 K)				(519)[b]		(158)[b]
PP	20	7	460.7	711.8	127.5	50.6
(10–460 K)				712.8 (714)[c]		100.5 (91)[c]
PET	51	15	553	544.7	48	48
(5–250 K)				(586)[d]		(44)[d]
Selenium	0	3	494.2	383	72	72
(1.5–300 K)				(350)[e]		(98)[e]
Diamond	0	3	3830[f]	1721	1721	2131
(10–1100 K)	0	3	3830[f]			1880[g]
						(2050)[h]
Graphite	0	3	3950[f]	2571	932	6.0
(0.5–1500 K)	0	3	3950[f]		1878 (1370)[i]	0.02 (37.5)[i]
Fullerene, C_{60}	174	6	1000[j]	83.9	20.7	20.7
(4–40 K)						(53)[k]

[a] from Eq. (6), in the subsequent rows other equations are explored, values in parentheses are for comparison to literature
[b] from Eq. (11), [26]
[c] from Eq. (11), [27]
[d] from Eq. (11), [28]
[e] from Eq. (11), [21]
[f] sublimation temp.
[g] from Eq. (9)
[h] from Eq. (9), [7]
[i] from Eq. (14), [13]
[j] estimate given in [29]
[k] from Eq. (9), [30]

Experimental heat capacities for diamond and graphite were taken from the critical evaluation of the literature in Ref. [13]. The recommended data for C_p(exp) of C_{60} were taken from Refs [29–31) and the group vibration spectra from Refs [32, 33].

The total number of vibrators ($3N$) were separated into the number of group vibrations (N_{gr}) and skeletal vibrations (N_{sk}) as listed in Table 2. For example, polyethylene has a total of nine degrees of freedom per (CH_2–) repeating unit. Of these 7 were taken as group vibrations, and the remaining 2 are skeletal [4]. For graphite, diamond and selenium with one-atomic motifs, on the other hand, all of the normal modes are initially taken to be of the skeletal type. With fullerene, in contrast, the crystal motif is C_{60}, with all internal bonds similar to graphite. This leads to 174 group vibrations and 6 skeletal vibrations [29].

All results of the fittings with the ranges of temperature used are listed in Table 2. The calculated vibrational heat capacities C_V(calc) and C_p(calc) using the best-fit values of Θ_1, Θ_2 and Θ_3, are shown in Figs 4–10. The separate skeletal and

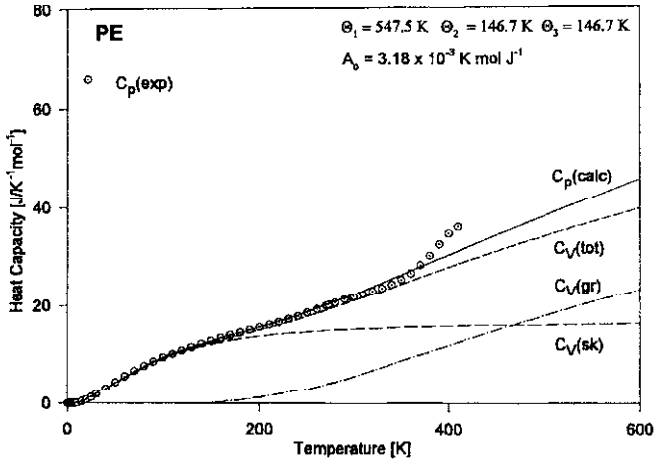

Fig. 4 Experimental and calculated heat capacities of crystalline PE with Eq. (6)

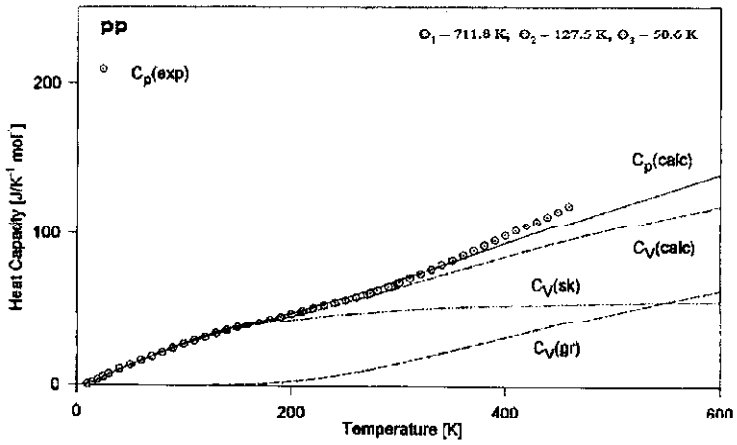

Fig. 5 Experimental and calculated heat capacities of crystalline PP with Eq. (6)

group contributions and the measured heat capacities C_p(exp) are also indicated. The RMS errors of the experimental data from the calculated values of C_p(calc) are always less than 3%, the usually assumed precision of the experimental data.

Discussion

The development of a detailed fit of the heat capacity of solids to an approximate function of the densities of vibrational states has gone through many stages of development. Until the present program was created, any laboratory interested in linking heat capacities to vibrational spectra had to develop rather extensive

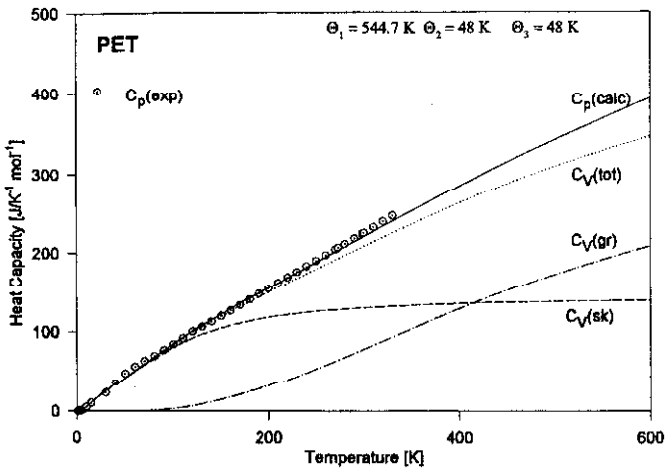

Fig. 6 Experimental and calculated heat capacities of crystalline PET with Eq. (6)

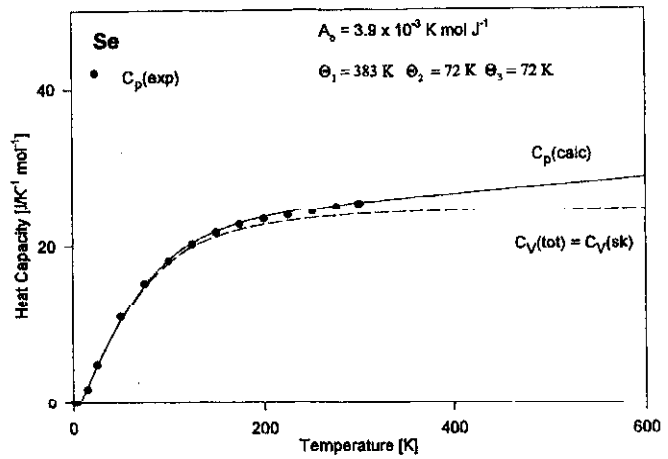

Fig. 7 Experimental and calculated heat capacities of trigonal Se with Eq. (6)

computational capabilities. The early discussions were based on manual computations based on tables of the Einstein [34], one- [4], two- [15], and three-dimensional [35] Debye funtions. This was followed by full main-frame computer programs for the inversion of heat capacity to the Tarasov parameters for polymers, Eq. (11) [11, 21]. Such inversions still needed empirical selection of the theta-temperatures and trial and error fitting, based on the constancy of the theta-temperatures over the analyzed temperature ranges, to be checked by subsequent error calculations. Recently a complete best fit resulting of Θ_1 and Θ_3 with respect to the smallest error in heat capacity was developed [22]. The here presented pro-

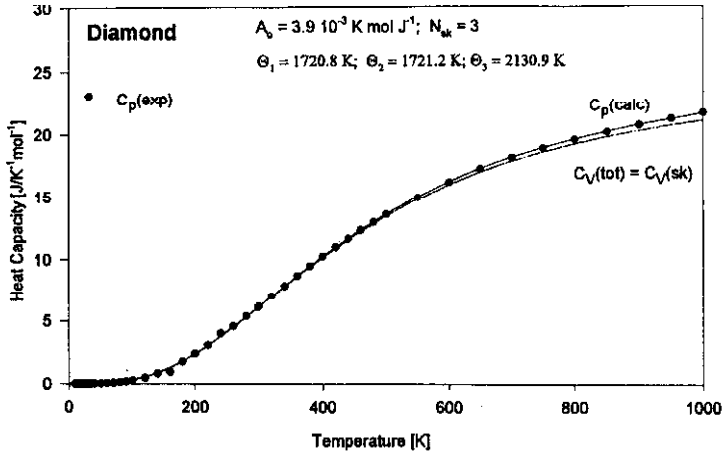

Fig. 8 Experimental and calculated heat capacities of diamond with Eq. (6)

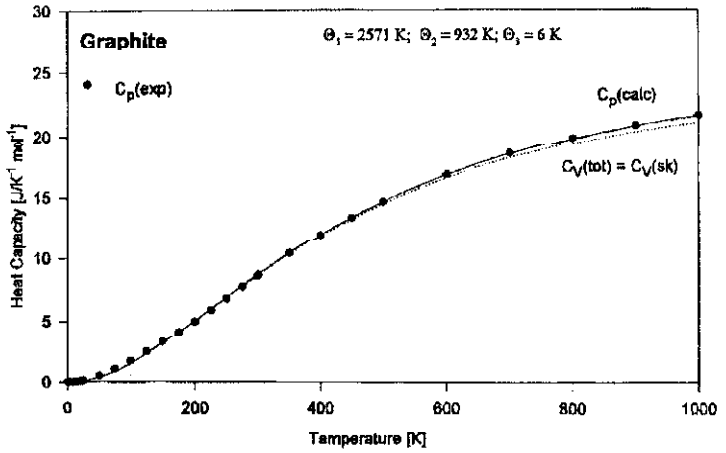

Fig. 9 Experimental and calculated heat capacities of crystalline graphite with Eq. (6)

gram, given in the Appendix, lets anyone with a modest investment in the Mathematica™ software do the fitting of heat capacities for any type of combinations of Tarasov, Debye, and Einstein models. It is hoped that this will make the quantitative interpretation of thermal analysis a much wider applied practice.

The meaning of the approximate vibrational spectra, as displayed in Figs 1 and 2, is obvious for the group vibrations (Figs 1A and B). The chosen approximations are to follow as closely as necessary the actual density of vibrational states. Above about 400 K, which corresponds to about 300 cm^{-1}, it becomes possible to approximate the detailed spectrum by box distributions and Einstein functions because the heat capacity *vs.* temperature curves increase in broadness with increasing frequency parameters. The often very precisely known group vibra-

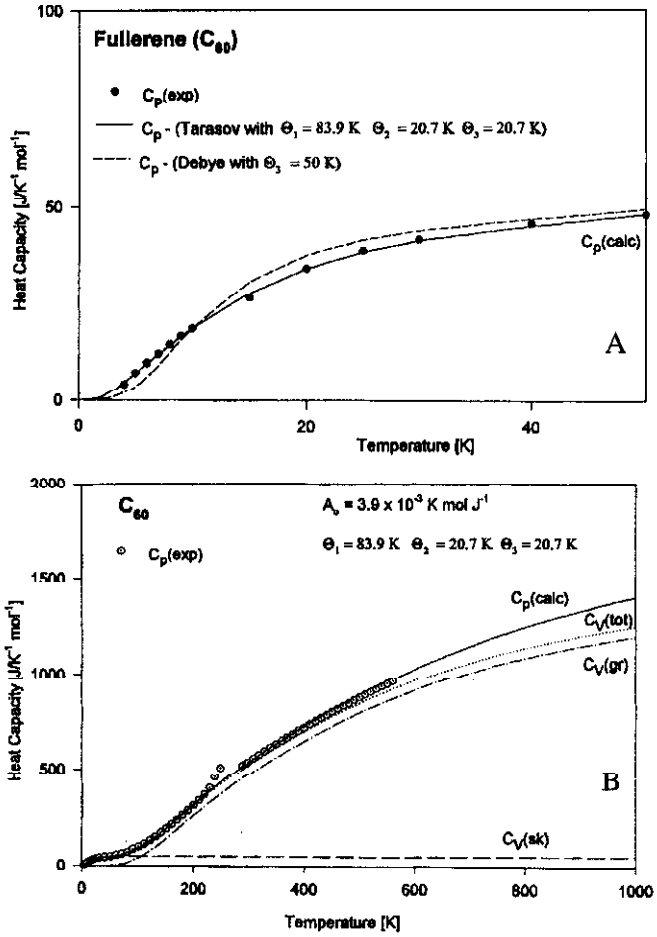

Fig. 10 Experimental and calculated heat capacities of fullerene with Eq. (6). (A) Low temperature data; (B) Complete temperature region

tional spectra can thus be simplified as shown in Figs 1A and 1B. Of the three Debye functions of Fig. 2 only the three-dimensional function (Fig. 2A) is known to match the low-frequency (acoustic) spectrum of crystalline solids. Its derivation is based on the assumption of an isotropic solid [6]. The more anisotropic the solid, the more does the actual frequency distribution deviate at higher frequencies from Fig. 2A. The method of separation of the group vibrations from the skeletal vibrations in Eq. (3) corrects for most of this anisotropy introduced by the chemical structure. The initial idea that the Figs 2B and C would similarly correspond to the molecularly two- and one-dimensional molecular structure is not verified, as pointed out earlier [13]. The atomic motion of layer structures and chains is in general not carried out in two and one dimension, and even the

strictly two- and one-dimensional vibrations show maxima at the high-temperature end of the distribution curves [2, 13]. Only the center part of the distributions of Figs 2B and C can, thus, be brought into good correspondence with the true spectra. The general Tarasov equation of Eq. (6) must thus be looked upon as a model that fits the lowest, three-dimensionally isotropic, acoustic vibrations (Debye's T^3 law of heat capacity at low temperatures) and approximates the higher, less isotropic frequencies with a ramp and a box distribution under the special rules that fix the number of vibrators:

$$N_1 = N_{sk}\left[1 - \frac{\Theta_2}{\Theta_1}\right]$$

$$N_2 = N_{sk}\left[\frac{\Theta_2}{\Theta_1} - \frac{\Theta_3^2}{\Theta_1\Theta_2}\right] \qquad (13)$$

$$N_3 = N_{sk}\left[\frac{\Theta_3^2}{\Theta_1\Theta_2}\right]$$

It is of interest to note by inspection of Table 2 how the frequency range of the three-dimensional Debye function decreases with increasing asymmetry of bonding. A final remark concerns the long-known deviation of the low-temperature heat capacities of amorphous solids from three-dimensional Debye functions [36]. Plots of heat capacity of polyethylene *vs.* crystallinity in the temperature region from 0 to 10 K lead for perfect crystals to a constant Debye temperature. For the glassy polymer, this is not the case. Attempts have been made to introduce a small number of additional low-frequency modes to account for the deviations. This is, however, an empirical fitting. Since these deviations occur in a temperature region where the skeletal heat capacity is already very small (less than 0.5 J K^{-1} mol^{-1} for PE below 10 K), the error caused forcing a fit to a constant theta temperature does not have a significant influence on the thermodynamic functions at higher temperature outside of a somewhat larger average error in heat capacity.

The analyses of the linear macromolecules presented in Table 2 show that the best fit to the general Eq. (6) has often a unique result: $\Theta_1 \neq \Theta_2 = \Theta_3$, precisely the assumption made in the derivation of the standard Tarasov equation for polymers, Eq. (11). Good examples are the data shown for crystals of PE, PET and polymeric Se (the trigonal allotrope) in Figs 4, 6, and 7. This justifies the use of the standard Tarasov approach to analyze the heat capacity of polymers, as done in the ATHAS data bank [9, 12]. The new, calculated values of Θ_3 and Θ_1 are usually in good agreement with those which were found by trial and error with Eq. (11). Similar good fits could also be achieved using a neural network, trained using a wide range of computed data based on Eq. (11) [37].

Occasional efforts to increase the number of fitting parameters by introducing different theta-temperatures for longitudinal and transverse vibrations or by introducing variable numbers of vibrators in the different parts of the Tarasov function do usually not give sufficient improvement of the calculations to warrant the extra effort [9, 36]. Naturally, knowledge of a more precise frequency spectrum would be preferable to the models involving Tarasov functions, but sufficiently accurate spectra are presently neither available by computation nor by analysis of Raman, infrared, or neutron data. For simple, linear macromolecules such complete computation of the vibrational heat capacity are presently only of use for higher temperatures, usually above about 100 K.

For some polymers, such as crystalline PP shown in Fig. 5, the standard Tarasov equation [Eq. (11)] does not fit as well as the general Tarasov equation [Eq. (6)]. Table 2 shows values of Θ_2=127 K, Θ_1=711.8 K, and Θ_3=50.6 K. This indicates that there are larger deviations from the box-like distribution of Eq. (11). One can speculate that the added concentration of low-frequency modes, accounted for by the two-dimensional Debye function seen in Fig. 1C, arise from the torsional oscillation of the $-CH_3$-group that was included in the skeletal vibrations of PP [27]. The consistency of both data sets can be seen from Eq. (12). Both treatments give similar Debye temperatures Θ_D. The fit of Eq. (6) gives 166 K, that of Eq. (11) 193 K.

Diamond is an example of a solid that contains strong bonds extending in all three directions of space. Therefore, one expects that the simple Debye approximation should lead to a good description of the total heat capacity. Fitting Θ_D to the experimental heat capacity yields 1880 K. The literature value for this type of fit, given in Table 2 [7], resulted from a fit to the heat capacity at about 1000 K ($\approx 0.5\Theta_D$). The result from Eq. (6) is $\Theta_1=\Theta_2\neq\Theta_3$, as shown in Table 2. This seems surprising, and suggests that some vibrations of the diamond lattice may be distributed as in a two-dimensional continuum. To gain more insight, we have constructed the approximate vibrational spectrum. The result is shown in Fig. 11 together with a normal-mode calculation from the literature [38, 39]. The initial shape of the density of states $\rho(\nu)$ is in both cases that of a three-dimensional continuum, i.e. $\rho(\nu)$ is proportional to the square of the frequency. The exact Θ^2 dependence extends from zero to Θ_2. This is followed by the difference of the remaining Θ^2-dependence and a two-dimensional Θ-dependence from Θ_2 to Θ_3. Note that, in contrast to Fig. 1C for which $\Theta_3<\Theta_2<\Theta_1$, in the diamond case the best fit yields $\Theta_3>\Theta_2=\Theta_1$. Therefore, from Eq. (13) one gets: N_1=0, N_2=–1.60, and N_3=4.60. The two-dimensional frequency distribution $\mathbf{D}_2(\Theta_3/T)$ in Eq. (6) extends from 0 to Θ_3 and is normalized to 4.6 moles of vibrators. On subtraction, it cancels the heat capacity contribution of the 3.0 moles of two-dimensional vibrators between 0 and Θ_2[$\mathbf{D}_2(\Theta_2/T)$] and results in the negative N_2 and the reduction from the $\mathbf{D}_3(\Theta_3/T)$ contribution seen in Fig. 11. The Tarasov fit has, thus, a minimum in its frequency distribution, similar to the normal mode calcu-

lation. Although the details of the frequency distribution are not fully reproduced, a considerably better approximation of the heat capacity than the simple Debye approximation is seen in Fig. 8. From inspection of the chemical structure of diamond it is obvious that the high-frequency maximum in the densities of vibrational states results from the C–C-stretching vibrations which couple only to a limited degree because of their close-to-90° bond angle.

Graphite is of interest to the discussion of heat capacities because of the unique layer structure of the crystals. While the carbon atoms within the planes of graphite are strongly bound, the adjacent planes are bound very weakly. If one assumes that the layer structure behaves like a two-dimensional continuum, one might expect that $\Theta_1=\Theta_2\neq\Theta_3$ in the general Tarasov equation [Eq. (6)]. Such analyses were done earlier for graphite [13] and some chalcogenides [15] using the appropriate Tarasov function:)

$$C_V(\mathrm{sk})/NR = \mathbf{T}(\Theta_2/T,\Theta_3/T) = \mathbf{D_2}(\Theta_2/T)-(\Theta_3/\Theta_2)^2[\mathbf{D_2}(\Theta_3/T)-\mathbf{D_3}(\Theta_3/T)] \quad (14)$$

Fitting Eq. (14) to the experimental data leads with the present software to the characteristic temperatures $\Theta_1=\Theta_2=1878$ K, and $\Theta_3=0.02$ K, somewhat different from the previous calculations (see Table 2) [13]. Equation (8) alone would accordingly also give an acceptable representation of the heat capacity data. When using Eq. (6), we obtain $\Theta_1=2571$ K, $\Theta_2=932$ K, and $\Theta_3=6$ K with a much better fit of the calculated heat capacities (see Fig. 9). A more detailed comparison with a normal mode calculations [39] was given earlier, and indeed, there exists a wide range of a box-like spectrum terminating at about 2400 K, in agreement with the stronger bonds within the planes of the graphite when compared to diamond.

A completely different crystalline allotrope of carbon is fullerene, C_{60}. It is a 'small' molecule with intramolecular bonding similar to graphite. The intermo-

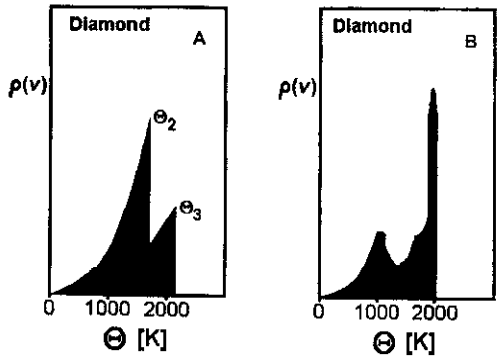

Fig. 11 Frequency spectra of diamond. (A) As obtained from Eq. (6); (B) Normal mode calculation [38]

lecular interactions can be derived when making the C_{60} molecules the motifs of the crystal. A fit of the experimental heat capacity from 4–40 K with the standard three-dimensional Debye Eq. (9) with six degrees of freedom and treating the intramolecular vibrations as group vibrations, available from normal mode calculations [41], leads to Θ_3=50 K. This is in good agreement with the results from a previous estimation of Θ_3=53 K [29–31]. Using Eq. (6), the result for the skeletal vibrations is $\Theta_1 \neq \Theta_2 = \Theta_3$, as shown in Table 2. From Eq. (13) one finds that around 1.5 normal-modes contribute to the Θ^2 distribution and the remaining 4.5 vibrators are best described by a constant frequency distribution. Figure 10A shows the improvement over the simple Debye function. Figure 10B shows the total heat capacity with an indication of the disordering transition that leads to a plastic crystal above about 260 K [32]. Equation (6) brings thus a considerable improvement to the low-temperature data. Between 0 and 50 K C_{60} has a much higher heat capacity than graphite and diamond, see Fig. 5 in Ref. [31]. Equation (12) shows that Θ_D is lowest for C_{60} (33 K) due to the large mass of the motif. This is followed by Θ_D for graphite (243 K) which develops skeletal vibrations within the plane, and for diamond Θ_D increases to 1848 K because of the extension of strong bonds in all directions. At higher temperature the heat capacities of the carbon allotropes are increasingly governed by the strong chemical bonds, of which diamond bonds are weaker than those of graphite and C_{60}. At about 1000 K the heat capacity of diamond increases, accordingly, above that of the fullerene and graphite. Ultimately, one expects that all allotropes of carbon reach a heat capacity of $3R$ (Dulong Petit's rule).

In conclusion, a fit of the general Tarasov equation [Eq. (6)] with the offered computer program can describe heat capacities of widely-different, solid materials (Figs 4–10). The presented discussion shows that the low-temperature approximation of Eq. (6) and its last term duplicate the Debye T^3-law and have a theoretically sound basis. The second and third parts of Eq. (6) are useful averages for the mid-frequency ranges of linear and planar vibrators which can improve the representation of low-temperature heat capacities. With a separate accounting for the group contributions, the vibrational heat capacity at constant volume can be represented over a wide temperature range. Only up to three theta-temperatures are needed to be fit to experimental data. The computer programs for analysis are now easily available [17].

* * *

This work was supported by the Division of Materials Research, National Science Foundation, Polymers Program, Grant # DMR 90-00520 and the Division of Materials Sciences, Office of Basic Energy Sciences, U.S. Department of Energy at Oak Ridge National Laboratory, managed by Lockheed Martin Energy Research Corp. for the U.S. Department of Energy, under contract number DE-AC05-96OR22464.

Appendix

Introduction

Text: This is a direct printout with Matematica(TM). Comments are given in the "Text:" (inactive cell's brackets). The bold lines in courier font are the program (active cell's brackets), the rest are the output printed by the program on runing. All examples are chosen to fit polyethylene. The program can be downloaded from our web-site.

Initialization

```
Text: Define a function to write the output Lists to an external file
listtoout[l_List] := StringJoin [StringReplace [ToString [NumberForm [1, 5]],
                     {"{"->"", "}"->"",","->"      "}],"\n"]
Text: Define a function to round numbers to n digits after the decimal point
round [x_,n_] := N[Round [x 10^n]/10^n];
roundc [x_] := round [x,4];
Text: Calculate the one-, two-, and three-dimensional Debye functions in terms of the polyloga-
rithm (Jonquiere's ε) functions and the Riemann zeta function [Eqs (7–9), a=Q1/T, Q2/T, Q3/T,
y=Q/T, Q=Theta, E=exp].
Dint1 = Expand [1/a Integrate [y^2 E^y/(E^y-1)^2, {y, 0, a}]]
```

$$-a+\frac{a}{1-E^a}-\frac{Pi^2}{3a}+2\mathrm{Log}[1-E^a]+\frac{2\mathrm{PolyLog}[2,E^a]}{a}$$

```
Dint2 = Expand [2/a^2 Integrate [y^3 E^y/(E^y-1)^2. [y. 0. a]]]
```

$$-2a+\frac{2a}{1-E^a}+6\mathrm{Log}[1-E^a]+\frac{12\mathrm{PolyLog}[2,E^a]}{a}-\frac{12\mathrm{PolyLog}[3,E^a]}{a^2}+\frac{12\mathrm{Zeta}[3]}{a^2}$$

```
Dint3 = Expand [3/a^3 Integrate [y^4 E^y/ (E^y-1)^2, {y, 0, a}]]
```

$$-3a+\frac{3a}{1-E^a}-\frac{4Pi^4}{5a^3}+12\mathrm{Log}[1-E^a]+\frac{36\mathrm{PolyLog}[2,E^a]}{a}-$$

$$-\frac{72\mathrm{PolyLog}[3,E^a]}{a^2}+\frac{72\mathrm{PolyLog}[4,E^a]}{a^3}$$

```
Text: These results are used to define the Debye functions for further calculations (change a to x)
D1[x_] := Dint1 /. a->x;
D2[x_] := Dint2 /. a->x;
D3[x_] := Dint3 /. a->x;
Text: Define names of the input (data.dat, datafe.dat, datafb.dat), auxiliary, and output (chi3d.dat,
dres.dat, dev.dat) data files, all as ASCII files. In some cases (for example in Mathematica for DOS
and MS WINDOWS), it is necessary to specify the full path of the files (for example:
datafile="C:\math\data.dat", experimental heat capacity, two column, temperature and heat capac-
ity; datafe.dat=Einstein frequency file, datafb.dat=box frequency file, chi3d.dat is the file of chi-
square as a function of Q1 and Q3=Q2; dres.dat is the file of results for all calculated heat capacities;
dev.dat is a file of the comparison of experimental and calculated heat capacity with the deviation
error.
datafile = "C:\math\data.dat";
freqEfile = "C:\math\datafe.dat";
freqBfile = "C:\math\datafb.dat";
chi3d = "C:\math\chi3d.dat";
```

```
dresfile = "C:\math\dres.dat";
devfile = "C:\math\dev.dat";
```

Read the experimental data and set up the computation parameters

Text: Read and plot the experimental data for the temperature dependence of the heat capacity from the input ASCII datafile, where the data are given in two-column format [T, Cp(exp)].

```
Cpexp = ReadList [datafile, {Number, Number}];
pcpe = ListPlot [Cpexp, PlotStyle->PointSize[.015]];
```

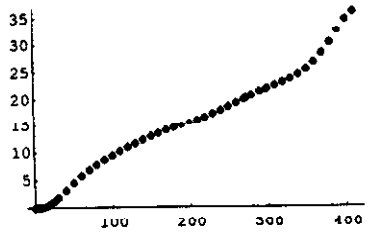

Text: Select the temperature range which is to be used in the calculation of the theta – temperatures Q1, Q2 and Q3

```
Tmin = 0;
Tmax = 270;
Cprange = Select [Cpexp, GreaterEqual [Tmax, First [#] [&];
Cprange = Select [Cprange, LessEqual [Tmin, First [#] [&];
```

Text: Number of skeletal vibrational modes

```
Nsk = 2;
```

Text: Melting temperature (in Kelvin)

```
Tmelt = 414.6;
```

Text: Gas constant R and the constant A0 in the Nernst-Lindemann equation [Eq. (1)]

```
Rc = 8.3143;
A0c = 3.18*10^-3;
const = {R->Rc, A0->A0c, Tm->Tmelt};
```

Text: Read the data for the part of the group vibration spectrum approximated by the Einstein model. The input ASCII file is freqEfile, where the data are given in two-column format: the frequency in Kelvin and the number of the corresponding normal modes in moles per repeating unit [QE, NE].

```
freqE = ReadList [freqEfile, {Number, Number}];
```

Text: Read the data for the part of the group vibration spectrum contributing as Cv(box). The input ASCII file is freqBfile, where the data are given in three-column format: the lower and the upper frequency of the box, and the number of the corresponding normal modes [QL, QU, N(gr)].

```
freqB = ReadList [freqBfile, {Number, Number, Number}];
```

Calculation of the skeletal contribution to Cv

Text: Convert the experimental data for Cp to those for Cv using Nernst-Lindemann equation [Eq. (1)]

```
Cvexp = {};
For [i=1, i<=Length [Cprange], i++,
    ClearAll [cvcur];
    cpcur = Cprange[[i]][[2]];
    eq = (cvcur (cpcur - cvcur) ==
        3R A0 Cprange[[i]][[1]]/Tm cpcur^2);
```

```
    eq = eq /. const;
    sol = NSolve[eq, cvcur];
    cadd = cvcur /. sol [[2]];
    Cvexp = Append [Cvexp, {Cprange[[i]][[1]], cadd}]
  ];
Text: Calculate and subtract the group heat capacity contributions to Cv [Eqs. (2–5)]]
CvEf = 0;
For [i=1, i<=Length [freqE], i++,
    TE = freqE[[i]][[1]];
    NE = freqE[[i]][[2]];
    cEcur = NE Rc (TE/T)^2 Exp [TE/T]/(Exp [TE/T]-1)^2;
    CvEf = CvEf + cEcur
  ];
CvBf = 0;
For [i=1, i<=Length [freqB], i++,
    QL = freqB[[i]][[1]];
    QU = freqB[[i]][[2]];
    NB = freqB[[i]][[3]];
    cBcur = NB Rc QU / (QU-QL) (D1[QU/T] - QL/QU D1 [QL/T]);
    CvBf = CvBf + cBcur
  ];
CvBf = Re [N[CvBf]];
Csdat = {};
For [i=1, i<=Length [Cvexp], i++,
    temp = Cvexp[[i]][[1]];
    cvcur = Cvexp[[i]][[2]];
    cvgrup = (CvEf /. T->temp) + (CvBf /. T->temp);
    csdatr = cvcur - cvgrup;
    Csdat = Append [Csdat, {temp, csdatr}]
  ];
Text: Plot the resulting skeletal heat capacity contribution to Cv as a function of temperature
cmax = Max[Map[Last, Csdat]];
cmax = cmax + .07 cmax;
pd = ListPlot[Csdat, PlotRange->{{Tmin, Tmax}, {0, cmax}},
    PlotStyle->PointSize[.015]];
```

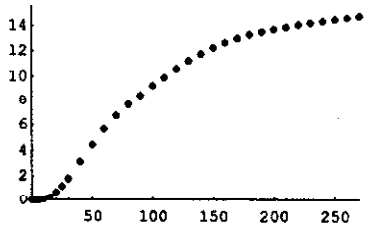

Fit the skeletal Cv(sk) to the Tarasov equation

```
Text: Define the general Tarasov function [Eq. (6)]
tarCs = D1[Q1/T] - (Q2/Q1) (D1[Q2/T] - D2[Q2/T]) -
      (Q3^2/Q1/Q2) (D2[Q3/T] - D3[Q3/T]);
tarCs = N[Nsk Rc tarCs];
tarCs = Re[Simplify[tarCs]];
Text: Define the chi-square statistical function [Eq. (10)]
chisq = 0;
```

```
For [i=1, i <=Length[Csdat], i++,
    cdati = Csdat [[i]];
    chisq = chisq + (cdati [[2]] - (tarCs /. T->cdati [[1]]))^2
  ];
```

Text: Minimize the chi-square function with respect to the Debye temperatures Q1, Q2 and Q3

```
fit = FindMinimum [chisq, {Q1, 100, 600}, {Q2, 100, 600}, {Q3, 100, 600}
AccuracyGoal >10, PrecisionGoal->10, MaxIterations->60]
{0.328011, {Q1 -> 547.457, Q2 -> 146.745, Q3 -> 146.745}}
```

Text: The first number above gives the minimal value of the chi-square function, which is achieved for the listed values of Q1, Q2 and Q3. These are the values of the best fit of the experimental data to the Tarasov function.

```
fit = fit[[2]];
auxchi = chisq /. Q2->Q3;
ContourPlot [auxchi, {Q1, 500, 600}, {Q3, 50, 250},
            ContourShading ->False];
```

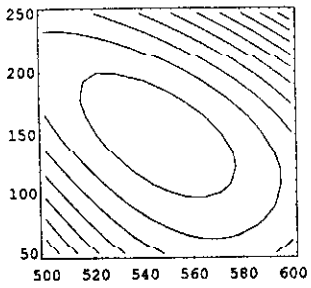

Text: The data for the dependence of the auxiliary function auxchi (chi-square as a function of Q1 and Q3=Q2) optionally can be written to file chi3d for further analysis.

```
str = OpenWrite [chi3d];
For [i=0, i <=20, i++,
For [j=0, j <=20, j++,
    q1 = 500 + i (600–500) /20.;
    q3 = 50 + j (250–50) /20.;
    res = auxchi /. {Q1->q1, Q3->q3};
    dat = {q1, q3, res};
    WriteString [str, listtoout dat]]
  ]];
Close [str];
```

Text: Plot the Tarasov function with the calculated values of Q1, Q2 and Q3, and compare it with the experimental data for the skeletal heat capacity Cv

```
pf = Plot [ (tarCs /. fit), {T,.1, Tmax},
    DisplayFunction->Identity];
Show [pd, pf];
```

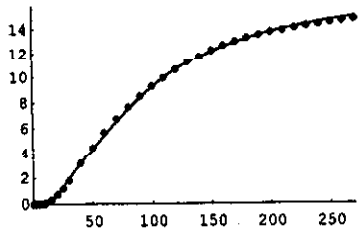

Calculation of the total heat capacity at constant pressure

Text: Calculate the total heat capacity Cv(tot) and convert it into the heat capacity Cp(calc) at constant pressure using the Nernst-Lindemann equation [Eq. (1)]

```
Cvtot = (tarCs /. fit) + CvEf + CvBf;
mian = 1 + Sqrt [1 - 12 AO R T/Tm];
Cptot = 2 Cvtot/mian;
Cptot = Cptot /. const;
```

Text: Plot the total heat capacity Cp(calc) and compare it with the measured data

```
pcp = Plot [Cptot, {T, 0.1, Tmax}, DisplayFunction->Identity];
cpmax = Max[Map[Last, Cprange]];
cpmax = cpmax + .07 cpmax;
Show [pcpe, pcp, PlotRange-> {{Tmin, Tmax}, {0, cpmax}};
```

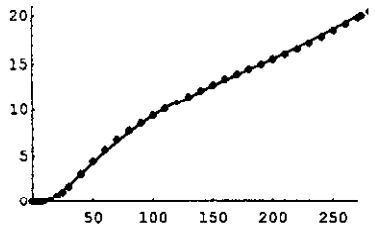

Tabulate and save the results

Text: Prepare a table of the calculated contributions to the heat capacity. Use the temperature interval dT1 for temperatures below T1, the interval dT2 for temperatures between T1 and T2, and the interval dT3 for temperatures between T2 and T3.

```
dT1 = 1;
T1 = 10;
dT2 = 5;
T2 = 50;
dT3 = 50;
T3 = 1000;
tab = {{Temp, Skelt, Einst, Box, Group, Cv, Cp}};
tt = dT1;
While [tt < T1,
        skel = roundc [(tarCs /. fit)/. T->tt];
        ein = roundc [CvEf /. T->tt];
        box = roundc [CvBf /. T->tt];
        group = roundc [ein+box];
        cvtt = roundc [skel+group];
        cptt = roundc [Cptot /. T->tt];
        tab = Append [tab, {tt, skel, ein, box, group, cvtt, cptt}
        tt = tt + dT1
       ];
tt = T1;
While [tt < T2,
        skel = roundc [ (tarCs /. fit)/. T->tt];
        ein = roundc [CvEf /. T->tt];
        box = roundc [CvBf /. T->tt],
        group = roundc [ein+box];
        cvtt = roundc [skel+group];
```

```
        cptt = roundc [Cptot /. T->tt];
        tab = Append [tab, {tt, skel, ein, box, group, cvtt, cptt}]
        tt = tt + dT2
       ];
tt = T2;
While [tt <= T3,
        skel = roundc [(tarCs /. fit)/. T->tt];
        ein = roundc [CvEf /. T->tt];
        box = roundc [CvBf /. T - >tt];
        group = roundc [ein+box];
        cvtt = roundc [skel+group];
        cptt = roundc [Cptot /. T ->];
        tab = Append [tab, {tt, skel, ein, box, group, cvtt, cptt}]
        tt = tt + dT3
       ];
TableForm [N[tab, 5]]
```

Temp	Skelt	Einst	Box	Group	Cv	Cp
1.	0.0001	0	0	0	0.0001	0.0001
2.	0.0009	0	0	0	0.0009	0.0009
3.	0.003	0	0	0	0.003	0.003
4.	0.007	0	0	0	0.007	0.007
5.	0.0137	0	0	0	0.0137	0.0138
6.	0.0237	0	0	0	0.0237	0.0238
7.	0.0377	0	0	0	0.0377	0.0378
8.	0.0563	0	0	0	0.0563	0.0564
9.	0.0801	0	0	0	0.0801	0.0803
10.	0.1098	0	0	0	0.1098	0.1101
15.	0.3625	0	0	0	0.3625	0.3635
20.	0.7899	0	0	0	0.7899	0.7929
25.	1.3396	0	0	0	1.3396	1.346
30.	1.9473	0	0	0	1.9473	1.9586
35.	2.5709	0	0	0	2.5709	2.5884
40.	3.1895	0	0	0	3.1895	3.2143
45.	3.7945	0	0	0	3.7945	3.8277
50.	4.3831	0	0	0	4.3831	4.4259
100.	9.2496	0.0076	0.0049	0.0125	9.2621	9.4463
150.	12.164	0.1366	0.1316	0.2682	12.432	12.811
200.	13.757	0.5685	0.675	1.2435	15.	15.623
250.	14.661	1.3769	1.7493	3.1262	17.787	18.73
300.	15.208	2.5292	3.2079	5.7371	20.945	22.308
350.	15.559	3.9231	4.8316	8.7547	24.314	26.205

400.	15.797	5.4458	6.4499	11.896	27.692	30.215
450.	15.964	7.0118	7.9636	14.975	30.939	34.193
500.	16.086	8.569	9.3284	17.897	33.983	38.061
550.	16.177	10.09	10.533	20.623	36.801	41.796
600.	16.248	11.562	11.585	23.147	39.394	45.401
650.	16.303	12.978	12.497	25.475	41.779	48.894
700.	16.347	14.336	13.288	27.623	43.971	52.302
750.	16.383	15.633	13.973	29.605	45.989	55.652
800.	16.412	16.868	14.567	31.435	47.848	58.972
850.	16.437	18.041	15.085	33.126	49.563	62.296
900.	16.457	19.151	15.538	34.689	51.146	65.66
950.	16.475	20.199	15.934	36.133	52.608	69.108
1000.	16.49	21.187	16.283	37.47	53.96	72.698

```
Text: Write data from the above table into ASCII file dresfile
str = OpenWrite [dresfile];
For [i=2, i<= Length [tab], i++,
    dat = tab [[i]];
    WriteString [str, listtoout [dat]]
   ];
Close [str];
Text: Plot the data together with all the measured values of Cp
all = Plot [{ (tarCs /. fit), (CvEf+CvBf), (Cvtot /. fit), Cptot
{T,.1, T3}, DisplayFunction->Identity];
Show [pcpc, all];
```

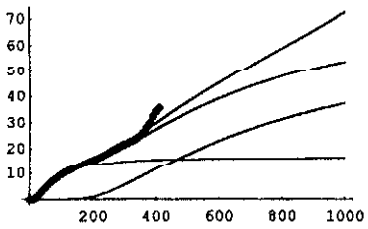


```
Text: Compare the measured and calculated values of Cp for temperatures below Tmax and
      calculate the standard deviation
mean = 0;
stddev = 0;
tabl = {{"Temp", "Cpexp", "Cpcalc", "Dev [%]"}};
ndat = Length [Cprange];
For [i=1, i<=ndat, i++,
    cpdc = Cpexp [[i]];
    teor = Cptot /. T->cpdc [[1]];
    devb = round [cpdc [[2]], 3]-round [teor, 3];
```

```
    dev = devb/teor 100;
    tab1 = Append [tabl, {cpdc [[1]], round [cpdc [[2]], 3],
          round [teor, 3], round [dev, 3]}];
    mean = mean + cpdc [[2]];
    stddev = stddev + (devb)^2
   ];
tab1 = N[tab1, 5];
TableForm [tab1]
```

Temp	Cpexp	Cpcalc	Dev [%]
2.	0.001	0.001	0
4.	0.006	0.007	−14.204
6.	0.021	0.024	−12.621
8.	0.05	0.056	−10.645
10.	0.097	0.11	−11.813
20.	0.729	0.793	−8.071
30.	1.838	1.959	−6.178
50.	4.523	4.426	2.192
70.	6.829	6.655	2.615
90.	8.655	8.593	0.722
110.	10.202	10.227	0.244
130.	11.599	11.604	−0.043
150.	12.867	12.811	0.437
170.	14.003	13.937	0.474
190.	15.05	15.053	−0.02
210.	16.1	16.207	−0.66
230.	17.254	17.429	−1.004
250.	18.545	18.73	−0.988
270.	19.909	20.11	−0.999

```
Text: Write data from the above table into ASCII file devfile
str = OpenWrite [devfile];
For [i=2, i<= Length [tab1], i++,
     dat = tab1 [[i]];
     WriteString [str, listtoout dat]]
    ];
Close [str];
Text: Absolute standard deviation:
stddevv = Sqrt [stddev/ndat]
0.0830773
Text: Relative standard deviation in %:
meanv = mean/ndat;
relstddev = stddevv/meanv 100
1.38184
```

Distribution of the low frequency vibrations of the solid

```
{Q1f, Q2f, Q3f} = {Q1, Q2, Q3} /. fit;
Text: Define the 1-, 2-, and 3-dimensional densities of states for continuum models
rho1 = 1/Q1f;
rho2 = 2f/(Q1f Q2 f);
rho3 = 3f^2/(Q1f Q2f Q3f);
rho [fr_] :=0;
rho [fr_] := (rho3 /. f->fr) /; (fr <= Q3f);
rho [fr_] := (rho2 /. f->)fr /; ((fr > Q3f) && (fr <= Q2f));
rho [fr_] := rho1 /; ((fr > Q2f) && (fr <= Q1f));
Text: Plot the best-fit density of states
Plot [rho [x], {x, 0, (Q1f+.07 Q1f)}];
```

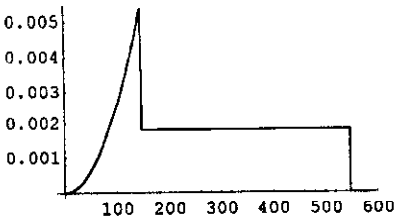

Text: End of program.

References

1 V. V. Tarasov, Compt. Rend. Acad. Sci. URSS, 46 (1945) 110.
2 W. H. Stockmayer and C. E. Hecht, J. Chem. Phys., 21 (1953) 1954.
3 M. Dole, Fortschr. Hochpol. Forsch., 2 (1960) 221.
4 B. Wunderlich, J. Chem. Phys., 37 (1962) 1207.
5 A. Einstein, Ann. Physik, 22 (1907) 180, 800.
6 P. Debye, Ann. Phys., 39 (1912) 789.
7 see for example E. Schrödinger, in H. Geiger and K. Scheel, eds, Handbuch der Physik, Vol. 10, Springer Verlag, Berlin 1926, p. 275.
8 M. Born and Th. von Kármán, Phys. Z., 13 (1912) 297; 14 (1915) 15.
9 B. Wunderlich, Pure and Appl. Chem., 67 (1995) 1919; for a detailed assessment of the method see: H. S. Bu, S. Z. D. Cheng and B. Wunderlich, J. Phys. Chem., 91 (1987) 4179.
10 V. V. Tarasov, Zh. Fiz. Khim., 24 (1950) 111.
11 S-F. Lau and B. Wunderlich, J. Thermal Anal., 28 (1983) 59.
12 For experimental data see: U. Gaur, H.-C. Shu, A. Mehta, S.-F. Lau, B. B. Wunderlich, M. Varma-Nair and D. Wunderlich, J. Phys. Chem. Ref. Data, 10 (1981) 89, 119, 1001, 1051; 11 (1982) 313, 1065; 12 (1983) 29, 65, 91; and 20 (1991) 349; and for fitted data check our WWW address on the Internet: http://funnelweb.utcc.utk.edu/~athas.
13 B. Wunderlich and H. Bauer, Adv. Polym. Sci., 7 (1970) 151.
14 V. V. Tarasov and G. A. Yunitskii, Zh. Fiz. Chim., 39 (1965) 2077.
15 U. Gaur, G. Pultz, H. Wiedemeier and B. Wunderlich, J. Thermal Anal., 21 (1981) 309.
16 S. Wolfram, The Mathematica: A System for Doing Mathematics by Compute, Addison-Wesley, Reading, MA 1995.
17 http://funnelweb.utcc.utk.edu/~athas.

18 Mathematica™ version 2.2 or higher, Wolfram Research, PO Box 6059, Champaign, IL 61826-6059; (Tel.: 1-800-441-MATH, email: info@wri.com).
19 W. Nernst and F. A. Lindemann, Z. Electrochem., 17 (1911) 817.
20 R. Pan, M. Varma-Nair and B.Wunderlich, J. Thermal Anal., 35 (1989) 955.
21 For computer programs and a general discussion of the Debye functions see: Yu. V. Cheban, S. F. Lau and B. Wunderlich, Colloid Polymer Sci., 260 (1982) 9.
22 G. Zhang and B. Wunderlich, J. Thermal Anal., 47 (1996) 899.
23 V. V. Tarasov, Dokl. Acad. Nauk. SSSR, 100 (1955) 307.
24 V. V. Tarasov, Compt. Rend. Acad. Sci. URSS, 54 (1946) 795.
25 V. V. Tarasov, Zh. Fiz. Khim., 27 (1953) 1430.
26 J. Grebowicz, H. Suzuki and B. Wunderlich, Polymer, 26 (1985) 561.
27 H. S. Bu, W. Aycock and B. Wunderlich, Polymer, 28 (1987) 1165.
28 S. Z. D. Cheng, S. Lim, L. H. Judovits and B. Wunderlich, Polymer, 28 (1987) 10.
29 Y. Jin, J. Cheng, M. Varma-Nair, G. Liang, Y. Fu, B. Wunderlich, X. D. Xiang, R. Motovoy and A. K. Zettl, J. Phys. Chem., 96 (1992) 5151.
30 B. Wunderlich and Y. Jin, Thermochim. Acta, 226 (1993) 169.
31 Y. Jin, A. Xenopoulos, J. Cheng, W. Chen, B. Wunderlich, M. Diack, C. Jin, R. Hettich, R. N. Compton and G. Guichon, Mol. Cryst., Liq. Cryst., 257 (1994) 235.
32 D. E. Weeks and W. G. Harter, J. Chem. Phys., 90 (1989) 4744.
33 R. E. Stanton and M. D. Newton, J. Phys. Chem., 92 (1988) 2141.
34 J. Hilsenrath and J. J. Ziegler, Tables of the Einstein Functions, Natl. Bur. Standards Monograph 49, Washington, 1962 [By now any programmable pocket calculator can compute Eq. (4) faster and to higher precision than one can look up a table].
35 J. A. Beattie, J. Math. Phys. (MIT), 6 (1926/27) 1.
36 J. E. Tucker and W. Reese, J. Chem. Phys., 46 (1967) 1388.
37 D. W. Noid, M. Varma-Nair, B. Wunderlich and J. A. Darsey, J. Thermal Anal., 37 (1991) 2295.
38 H. M. J. Smith, Phil. Trans., A241 (1948) 105.
39 W. V. Houston, Z. Naturforsch., 3a (1948) 607.
40 J. A. Young and J. V. Koppel, J. Chem. Phys., 42 (1965) 357.
41 D. E. Weeks and W. G. Harter, Chem. Phys. Lett., 137 (1988) 366.